The phenotype of peritoneal mouse macrophages depends on the mitochondria and ATP/ADP homeostasis

Wei Chen[1,2], Hector Sandoval[1,3], Jacek Z. Kubiak[4,5,6], Xian C Li[1,3] , Rafik M Ghobrial[1,3], Malgorzata Kloc*[1,3,7]

[1]Houston Methodist Research Institute, Houston, Texas, USA;
[2]Department of Nephrology, Second Xiangya Hospital, Central South University, Changsha 410011, China.
[3]Houston Methodist Hospital, Department of Surgery, Houston, Texas, USA;
[4]CNRS UMR 6290, Institute of Genetics and Development of Rennes, Cell Cycle Group, IFR 140 GFAS, France;
[5]University of Rennes 1, Faculty of Medicine, Rennes, France;
[6]Department of Regenerative Medicine, Military Institute of Hygiene and Epidemiology (WIHE), Warsaw, Poland;
[7]University of Texas, MD Anderson Cancer Center, Department of Genetics, Houston Texas, USA

Correspondence Address:

Malgorzata Kloc
Houston Methodist Hospital, Department of Surgery,
6550 Fannin St., Houston, TX 77030
Tel. 713.441.6875
Fax 713.790.3755
e-mail: mkloc@houstonmethodist.org

Abstract

Different macrophage subtypes have different morphologies/shapes and functions. Naïve M0 macrophages are elongated. Pro-inflammatory M1 that produce the bactericidal molecule iNos are round. Anti-inflammatory M2 macrophages that produce the pro-healing enzyme Arg-1 are highly elongated. We showed previously that the morphologies of M0 and M2 but not M1macrophages are RhoA-dependent. Macrophage-specific deletion of RhoA causes the extreme elongation (hummingbird phenotype) of M0 and M2 but not M1 macrophages. The M1 and M2 macrophages also differ in their metabolic status. Here, we studied the effect of the oxidative phosphorylation inhibitors, antimycin A and oligomycin A, at a suboptimal dose, which depolarizes mitochondria but does not eliminate mitochondrial functions, on the mitochondria/energy production and phenotype of wild-type and RhoA-deleted M0, M1 and M2 peritoneal mouse macrophages. We found that, while untreated M1 macrophages had the lowest and the M2 had the highest level of ATP the ATP/ADP ratio was nearly identical between M0, M1 and M2 macrophages. Inhibitor treatment resulted in approximately 60% increase in ATP level and ATP/ADP ratio in M0 and M2 macrophages, and decrease in the level of filamentous (F) actin, and these changes correlated with a drastic shortening/tail retraction of M0 and M2 macrophages, and decreased expression of Arg-1 in M2 macrophages. The treatment of M1 macrophages caused only a 30% increase in the ATP level and ATP/ADP ratio, and while it did not affect the shape of M1 macrophages, it increased the production of iNos. This indicates that the maintenance of mouse macrophage phenotypes depends on mitochondrial function and ATP/ADP homeostasis.

Key words: macrophage, metabolism, mitochondria, antimycin, oligomycin, RhoA, ATP

Introduction

Macrophages are very heterogeneous phenotypically, functionally and metabolically. Until recently it had been believed that energy production in inflammatory/anti-bacterial M1 macrophages relied mainly on aerobic glycolysis, while anti-inflammatory/healing M2 macrophages used oxidative phosphorylation (OXPHOS) (1). Although recent studies have shown that such a belief is a tremendous oversimplification and that both glycolysis, and OXPHOS play a role in shaping M1 and M2 phenotypes (2,3), the metabolic profile of M1 macrophages is related to their bactericidal activity and their production of the nitric oxide synthase iNos that kills intracellular pathogens, while the metabolic profile of M2 macrophages relates to the production of Arginase 1 (Arg-1) and its products, such as polyamines, ornithine and urea, which are involved in tissue repair and healing (1). It has also been shown that the inhibition of oxidative metabolism blocks the M2 phenotype and reverses the macrophage to the M1 state (4,5). We showed recently that the phenotype/morphology of M0 (slightly elongated), M1 (round) and M2 (highly elongated) macrophages depend on the actin cytoskeleton, which is regulated by the small GTPase RhoA pathway. We also showed that M0, M1 and M2 macrophages respond differently to RhoA pathway interference (6-9). The macrophage-specific deletion of RhoA or inhibition of RhoA/ROCK kinase disrupts the actin cytoskeleton and causes the extreme elongation (hummingbird) phenotype of M0 and M2 mouse macrophages. In contrast, RhoA-deleted M1 macrophages remain round or roundish/multipolar (6-9). It has also been shown that the mechanically enforced elongation of M0 macrophages induces the M2 phenotype (10). Several studies have shown that cell elongation requires the relocation of the mitochondria to the most energy-demanding regions of the cell where the most intense reorganization of the actin cytoskeleton occurs (11- 13). Thus, we were interested in if or how the disruption of mitochondrial function would affect the phenotype of M0, M1 and M2 macrophages. We studied the effect of suboptimal doses of the oxidative phosphorylation inhibitors antimycin A, which inhibits cytochrome c reductase (14-16), in conjunction with oligomycin A, which inhibits ATP synthase (14, 16, 17), on the phenotype of wild-type and RhoA-deleted MO, M1 and M2 macrophages. At suboptimal doses, these drugs depolarize the mitochondria but do not completely eliminate mitochondrial functions (18). We found that inhibitor treatment caused a statistically significant increase in the ATP level and ATP/ADP ratio in

M0 and M2 macrophages and a much smaller increase in M1 macrophages. Inhibitor treatment caused a dramatic shortening (tail retraction) of wild-type and RhoA-deleted (hummingbird phenotype) M0 and M2 macrophages and inhibited the expression of Arg-1 in M2 macrophages. In contrast, while inhibitor treatment did not have a noticeable effect on the morphology of M1 macrophages, it increased the expression of the M1 marker iNos. In addition, inhibitor treatment lowered the level of filamentous (F) actin in favor of the globular (G) actin. This suggests that macrophage shortening is a direct effect of deficiency of filamentous actin, which is necessary for cell elongation.

This indicates that the phenotypes of M0/M2 macrophages and M1 mouse macrophages have different requirements not only for RhoA pathway activity but also for mitochondrial function and ATP/ADP homeostasis. Further studies are needed to confirm if the human macrophages have the same requirements like mouse macrophages.

Material and methods

Animals

Breeding and all experiments were performed according to Methodist Hospital Research Institute's animal care and use NIH standards in concordance with the "Guide for the Care and Use of Laboratory Animals" (DHHS publication No. (NIH) 85-23 Revised 1985), the PHS "Policy on Humane Care and Use of Laboratory Animals" and the NIH "Principles for the Utilization and Care of Vertebrate Animals Used in Testing, Research and Training." All studies were performed according to the animal protocol AUP-0317-0006 (IS00003962) entitled "Tolerance Induction in a Rodent System" approved by Houston Methodist Institutional Animal Care and Use Committee. Mouse euthanasia was performed according to the HMRI Euthanasia of Rodents Procedure by isoflurane overdose via vaporizer inhalation, followed by cervical dislocation and thoracotomy to ensure death. For the genotyping, mice were anesthetized with 3-4 % isoflurane. RhoA$^{flox/flox}$ mice (a gift from Dr. Richard A. Lang from the UC Department of Pediatrics and UC Department of Ophthalmology, Cincinnati Children's Hospital, Cincinnati, Ohio) were crossbred with B6.129P2-Lyz2tm1(cre)Ifo/J mice (JAX® Mice (Bar Harbor, Maine, USA) to generate Lyz2$^{Cre+/-}$ RhoA$^{flox/flox}$ mice and genotyped as described in Liu et al. (9).

Peritoneal macrophages

Mouse peritoneal macrophages from no Cre-negative mice ($Lyz2^{Cre-/-}$ $RhoA^{flox/flox}$), hereafter called the wild-type, or RhoA deleted $Lyz2^{Cre+/-}$ $RhoA^{flox/flox}$ mice, further called the RhoA-KO, were purified. Mice around 8 weeks old were used. 3 mice were used for single experiment Mouse peritoneal cavity was injected three consecutive times with 8 ml of cold DPBS and after 1 min the peritoneal eluent was collected by centrifugation at 1700 rpm for 5 min. Cell pellet was re-suspended in 5-10 ml of Dulbecco's Modified Eagle Medium (DMEM) supplemented with 10% fetal bovine serum (FBS), 100U/ml penicillin and 100 µg/ml streptomycin and seeded in 12/24 well plates. Total number of cells from 3 mice was $3x10^6$. All media were from Thermo Fisher Scientific, Waltham, MA, USA. After overnight incubation at 37℃ and 5% CO□, plates were washed twice with DPBS to remove the non-adherent cells and incubated overnight. The total number of adherent cells was around 2-2.4 $x10^6$. For M1 polarization, macrophages were incubated for 24 hr with 20 ng/ml of recombinant murine IFN-γ (Peprotech, Rocky Hill, NJ, USA) and100 ng/ml of Lipopolysaccharide (LPS) (Sigma Aldrich,St. Louis, MO, USA). For M2 polarization, macrophages were incubated with 20 ng/ml of recombinant murine IL-4 (Peprotech) and 10 ng/ml of recombinant murine IL-13 (Peprotech) as described previously (6,7). For immunostaining macrophages were polarized and treated with inhibitors in glass bottom chamber slides at around $0.4x10^6$/slide.

Inhibitor treatment

Unpolarized wildt type and RhoA-KO M0 macrophages and macrophages polarized into the M1 and M2 phenotype (see polarization protocol above) were incubated for 24 hr in the presence of oligomycin A (ETC complex V inhibitor) at 10 µM final concentration and antimycin A (ETC complex III inhibitor) at 4µM final concentration. The total time of macrophage culture from the moment of isolation to the end of the experiment was 72 hours.

ATP/ ADP assay

ATP and ADP measurements were performed using the ApoSensor ADP/ATP Ratio Bioluminescent Assay kit (Biovision Inc., CA, USA) according to the manufacturer's protocol on M0, M1 and M2 macrophages after 72 hours of total time in culture.

Mitochondria visualization and Western blotting

For immunostaining of the mitochondria macrophages were seeded on chamber slides ($0.4x10^6$/slide). Control and treated macrophages were fixed in 4% formaldehyde in PBS with 0.05% Triton X100. After washing in PBS-Tween 20, fixed cells were blocked in casein blocking buffer (BioRad, USA) with 0.05% Tween 20 and subsequently incubated in blocking buffer with a 1:100 dilution of anti-COX4 antibody (cat # 459600, Invitrogen). After extensive washing in PBS-Tween 20, cells were incubated in blocking buffer with a 1:200 dilution of FITC –conjugated secondary antibody from ThermoFisher Scientific with Rhodamine-phalloidin (2µl of methanolic solution/500 ml) for several hours at room temperature. After extensive washing in PBS-Tween 20 cells were mounted in ProLong® Gold Antifade with DAPI from Fisher Scientific and observed under a Nikon fluorescence microscope.

All experiments were repeated 3-4 times.

G-actin/ F- actin assay

G-actin/ F- actin assay kit # BK037 was purchased from Cytoskeleton.Inc (USA). Peritonelam macrophages were isolated as described above and cultured Dulbecco's Modified Eagle Medium (DMEM) supplemented with10% FBS, 100U/ml penicillin and 100ug/ml streptomycin) at 37℃ and 5% CO2 for 24 hours. Subsequently macrophages were polarized for 24 hours toward M1 phenotype with 100ng/ml LPS and 20ng/ml IFN-r, and M2 phenotype with 20ng/ml IL-4 and 10ng/ml IL-13) and treated with 10µM oligomycin and 4µM antimycin overnight. Subsequently medium was aspirated and 100µl of warm LAS2 buffer (lysis and F-actin stabilization buffer with ATP solution and protease inhibitor cocktail) was added and cells were harvested into 1.5ml centrifuge tube. The lysate was incubated 37℃ for 10 min and centrifuged at 350x g at room temperature for 5min. The supernatant was transferred to centrifuge tube and centrifuged at 25,000g x g 37℃ for 2 h. The supernatant, which contains soluble G actin, was transferred to another tube and the pellet containing insoluble F actin was treated with 100µl of F-actin depolymerization buffer and incubated on ice for 1h, with pipetting up and down several times every 15minutes. Finally, the pellet and supernatant were mixed with 25µl of 5x SDS sample buffer, separated on a 12% SDS gel using standard electrophoresis and analyzed by Western blotting using Anti-Actin Rabbit Poly-clonal Antibody.

.

Results

Effects of mitochondrial inhibitors on macrophage morphology/elongation and distribution of mitochondria

To visualize the mitochondria, we stained macrophages with an antibody against the cytochrome c oxidase subunit 4 (Cox4). Cox4 is the mitochondrial inner membrane respiratory enzyme that participates in the transfer of electrons from cytochrome c to molecular oxygen (19).

The nonactivated/naïve, untreated macrophages were slightly elongated with pronounced front (containing the nucleus) and tail, and had the average length of 54± 9.1μm (Fig.1A, B, E). Immunostaining with a mitochondrial marker showed that the mitochondria (contacting each other/interconnected in the mitochondrial network (21, 20) were present around the nucleus and in the macrophage tail (Fig.1A, B). Antimycin and oligomycin treatment caused approximately 50% shortening of the M0 macrophages (average length of 21±2.9μm) and the elimination of the macrophage tail (Fig.1C, D, E). In inhibitor- treated M0 macrophages the mitochondria were located around the nucleus and instead of the interconnected mitochondrial network, clearly separated, round mitochondria were visible (Fig.1C, D). Untreated M1 macrophages were roundish (pancake-like) with the average length 31±5.6 μm, and with a pronounced network of interconnected mitochondria (Fig.2A, B, E). We always measured the length of the macrophages-in case of round macrophages the length was equal to the macrophage width. Although the antimycin and oligomycin treatment did not have any noticeable effects on macrophage shape or size (average length was 34±3.1μm; Fig. 2C, D, E) the mitochondrial network disappeared and separated, and round mitochondria were clearly visible (Fig.2C, D). Untreated M2 macrophages were highly elongated with the average length 104±31.6 μm, and the mitochondrial network was present around the nucleus, in the macrophage leading edge and in the tail (Fig. 3A, B, E). Similar to M0 macrophages, treatment with antimycin and oligomycin resulted in approximately 50% shortening of M2 macrophages (average length 40±9.8 μm) and the replacement of the mitochondrial network with

clearly separated, round mitochondria (Fig.3C, D, E). These results indicate that the inhibitor treatment similarly affected morphology of mitochondria in all macrophage subtypes. However, the effect on macrophage shape was limited to M0 and M2 macrophages. We also studied the effect of antimycin and oligomycin on the RhoA-deleted macrophages. We showed previously that RhoA-deletion causes the extreme elongation (hummingbird phenotype) of M0 and M2 macrophages and does not affect or has only a slight effect on M1 macrophages, which remain roundish or roundish/multipolar (6-9). The inhibitor treatment of RhoA-deleted macrophages, similar to the wild-type macrophages, resulted in the dramatic shortening of M0 and M2 macrophages (Fig. 4A, A1, B, B1), without much effect on M1 macrophages (Fig.4C, C1).

Effect of mitochondrial inhibitors on the expression of molecular markers and ATP/ADP homeostasis

The signature molecule crucial for the inflammatory function of M1 macrophage is nitric oxide synthase (iNos). Western blot analysis showed that the level of expression of iNos significantly increased in M1 macrophages treated with antimycin and oligomycin (Fig.4A, B). The signature molecule of the pro-healing, anti-inflammatory M2 macrophages is arginase 1 (Arg-1). Western blot analysis showed that treatment with antimycin and oligomycin significantly reduced expression of Arg-1 (Fig. 4A,C) in these macrophages. Although further studies are necessary to establish if the increase/decrease of the level of iNos/Arg-1 was caused by changes in protein translation or in protein stability or both, the changes in the expression of molecular markers correlated with the changes in ATP, ADP and ATP/ADP levels. The control, untreated M1 macrophages had the lowest level of ATP and ADP, and M2 macrophages had the highest level of ATP and ADP (Fig.5A, B). However, the ATP/ADP ratio was identical in untreated M0, M1 and M2 macrophages (Fig.5C). Treatment with antimycin and oligomycin caused decrease in ADP levels and increase in the ATP levels in all macrophage subtypes (Fig.5A, B). The ATP/ADP ratio, which was nearly identical in all subtypes of untreated macrophages, increased in inhibitor-treated macrophages. The largest increase occurred in M0 and M2 macrophages and the smallest in M1 macrophages (Fig.5C).

These findings indicate that the disruption of ATP/ADP homeostasis has a profound effect on the morphology/shape of M0 and M2 macrophages and the expression of signature proteins in M1 and M2 mouse macrophages.

Effect of mitochondrial inhibitors on G and F actin level

We assessed the level of globular (G) versus filamentous (F) actin in control and inhibitor treated macrophages. These analyses showed that treatment with inhibitors decreases level of F actin in favor of G actin especially in M1 and M2 macrophages (Fog.6 D, E). Because the polymerization of G actin into filamentous actin is necessary for cell elongation, the decreased F actin content may be directly responsible for the shortening of M0 and M2 macrophages after inhibitor treatment.

Discussion

We showed that the morphology of M0, M1 and M2 peritoneal mouse macrophages and the production of signature molecular markers of M1 and M2 macrophages, induced by polarization conditions described in Material and methods, depend on the integrity of the mitochondria and on ATP/ADP homeostasis. Several studies, including studies from our laboratory, have shown that mouse peritoneal and bone marrow-derived macrophages have a very distinct morphology: naïve M0 macrophages are elongated, M1 macrophages are roundish and M2 macrophages are highly elongated (6-10, 22 -24). We also showed recently that the morphology of M0 and M2 but not M1 macrophages depends on the small GTPase RhoA pathway, which is a master regulator of actin organization and polymerization (25). We showed that the macrophage-specific deletion of RhoA or inhibition of the RhoA downstream effector ROCK kinase with an Y27632 inhibitor induced extreme elongation (hummingbird phenotype) of M0 and M2 mouse peritoneal and bone marrow-derived macrophages without much effect on the morphology/shape of M1 macrophages (6-9). This indicated that the M0/M2 macrophage phenotype has different requirements for RhoA pathway activity than the M1 phenotype. It has been shown that actin polymerization and organization in various types of cells depend not only on the RhoA pathway but also on the distribution and proper function of mitochondria (11-13). The mitochondria deliver energy for actin polymerization, and during cell elongation or cell movement, the mitochondria relocate to the regions of the cell with the highest energy demands (3, 12, 13, 26). In all eukaryotic cells mitochondria constantly

divide and fuse into a dynamic interconnected mitochondrial network (27 - 31). The inter-mitochondrial contacts stabilize the individual mitochondria and by increasing the total mitochondrial volume, increase cellular respiration (32). The network of fused mitochondria is critical for the maintenance of the inner mitochondrial membrane potential and mitochondrial respiratory functions, and the cytochrome c release from mitochondria causes the disintegration and separation of the network into individual, small mitochondria (33). In this study, we showed that the treatment of macrophages with a suboptimal dose of the oxidative phosphorylation inhibitors antimycin and oligomycin caused disintegration of the mitochondrial network in M0, M1 and M2 macrophages and resulted in the disruption of ATP/ ADP homeostasis, and decrease in the level of filamentous (F) actin, which in turn caused the dramatic shortening of M0 and M2 (both wild-type and RhoA-deleted) macrophages and reduced the expression of M2 marker Arg-1. In contrast, the treatment did not have any obvious effect on the morphology/shape of M1 macrophages; however it increased the expression of the M1 marker iNos. We showed that although control M0, M1 and M2 macrophages differed in the ADP and ATP level, their ATP/ADP ratio was nearly identical. This indicates that the ATP/ADP ratio is tightly controlled and balanced to be the same no matter what is the macrophage subtype. The treatment with inhibitors ruins this balance and uncontrolled ATP/ADP ratio results in changes in macrophage morphology and protein expression pattern. In addition, our analysis of G (globular) and F (filamentous) actin content in control and inhibitor treated macrophages showed that inhibitors treatment decreased level of F actin in favor of G actin. Because, as we showed in our previous studies, macrophage elongation depends on actin polimerisation/ filamentous actin, this result strengthens the idea of causative relationship between changes in morphology, which depends on filamentous actin, ATP/ ADP ratio imbalance and mitochondria. Although further studies are necessary to establish which mechanisms and molecules are involved in the antimycin and oligomycin effects, the results indicate that the phenotypes of the M0/M2 macrophages versus the M1 macrophages have different requirements not only for RhoA pathway activity but also for mitochondrial function and ATP/ADP homeostasis. One has to remember that these results pertain to mouse macrophages in *in vitro* system and we do not know if/how they relate to human macrophages and the situation *in vivo*.

Acknowledgements

We are grateful for support from William Stamps Farish Fund and Donald D. Hammill Foundation.

References

1. Galván-Peña S, O'Neill LA. Metabolic reprograming in macrophage polarization. Front Immunol. 5 (2014), 420-426.

2. Huang SC, Smith AM, Everts B, Colonna M, Pearce EL, Schilling JD, Pearce EJ. Metabolic Reprogramming Mediated by the mTORC2-IRF4 Signaling Axis Is Essential for Macrophage Alternative Activation. Immunity. 45(2016):817-830.

3. Mehta MM, Weinberg SE, Chandel NS. Mitochondrial control of immunity: beyond ATP. Nat Rev Immunol. 2017 Jul 3. doi: 10.1038/nri.2017.66. [Epub ahead of print] Review.

4. Rodríguez-Prados JC, Través PG, Cuenca J, Rico D, Aragonés J, Martín-Sanz P, Cascante M, Boscá L. Substrate fate in activated macrophages: a comparison between innate, classic, and alternative activation. J Immunol. 185 (2010) 605-14.

5. Vats D, Mukundan L, Odegaard JI, Zhang L, Smith KL, Morel CR, Wagner RA, Greaves DR, Murray PJ, Chawla A. Oxidative metabolism and PGC-1beta attenuate macrophage-mediated inflammation. Cell Metab. 4 (2006) 13-24.

6. Liu Y, Chen W, Minze LJ, Kubiak JZ, Li XC, Ghobrial RM, Kloc M. Dissonant response of M0/M2 and M1 bone marrow derived macrophages to RhoA pathway interference. Cell Tissue Res. 366 (2016a) 707-720.

7. Liu Y, Minze LJ, Mumma L, Li XC, Ghobrial RM, Kloc M. Mouse macrophage polarity and ROCK1 activity depend on RhoA and non-apoptotic Caspase 3. Exp Cell Res. 341(2016b) 225-36.

8. Liu Y, Tejpal N, You J, Li XC, Ghobrial RM, Kloc M. ROCK inhibition impedes macrophage polarity and functions. Cell Immunol. 300 (2016c) 54-62.

9. Liu Y, Chen W, Wu C, Minze LJ, Kubiak JZ, Li XC, Kloc M, Ghobrial RM (2017) Macrophage/monocyte-specific deletion of RhoA down-regulates fractalkine receptor and inhibits chronic rejection of mouse cardiac allografts. JHLT. 36 (2017) 340-354.

10. McWhorter FY, Wang T, Nguyen P, Chung T, Liu WF. Modulation of macrophage phenotype by cell shape. Proc Natl Acad Sci U S A. 110 (2013) 17253-17258.

11. Boldogh IR, Pon LA. Interactions of mitochondria with the actin cytoskeleton. Biochimica et Biophysica Acta 1763 (2006) 450–462

12. Cunniff B, McKenzie AJ, Heintz NH, Howe AK. AMPK activity regulates trafficking of mitochondria to the leading edge during cell migration and matrix invasion. Mol Biol Cell. 27(2016), 2662-2674.

13. Schuler MH, Lewandowska A, Caprio GD, Skillern W, Upadhyayula S, Kirchhausen T, Shaw JM, Cunniff B. Miro1-mediated mitochondrial positioning shapes intracellular energy gradients required for cell migration. Mol Biol Cell. 28(2017):2159-2169.

14. Georgakopoulos ND, Wells G, Campanella M. The pharmacological regulation of cellular mitophagy. Nat Chem Biol. 13(2017):136-146.

15. Kalbácová M, Vrbacký M, Drahota Z, Melková Z. Comparison of the effect of mitochondrial inhibitors on mitochondrial membrane potential in two different cell lines using flow cytometry and spectrofluorometry. Cytometry A. 52(2003):110-6.

16. Smolina N, Bruton J, Kostareva A, Sejersen T. Assaying Mitochondrial Respiration as an Indicator of Cellular Metabolism and Fitness. Methods Mol Biol. 1601(2017) 79-87.

17. Martin JA, Martini A, Molinari A, Morgan W, Ramalingam W, Buckwalter JA, McKinley TO. Mitochondrial electron transport and glycolysis are coupled in articular cartilage. Osteoarthritis Cartilage. 20(2012):323-9.

18. Lazarou M, Sliter DA, Kane LA, Sarraf SA, Wang C1, Burman JL, Sideris DP, Fogel AI, Youle RJ. The ubiquitin kinase PINK1 recruits autophagy receptors to induce mitophagy. Nature. 524 (2015): 309-314

19. Zeviani M, Nakagawa M, Herbert J, Lomax MI, Grossman LI, Sherbany AA, Miranda AF, DiMauro S, Schon EA. Isolation of a cDNA clone encoding subunit IV of human cytochrome c oxidase. Gene. 55 (1987): 205–217.

20. Bereiter-Hahn J, Vöth M, Mai S, Jendrach M. Structural implications of mitochondrial dynamics. Biotechnol J. 3(2008):765-780.

21. Lackner LL. Shaping the dynamic mitochondrial network. BMC Biol. 12 (2014)35-45.

22. Geissmann F, Manz MG, Jung S, Sieweke MH, Merad M, Ley K. Development of Monocytes, Macrophages, and Dendritic Cells. Science 327(2010): 656-661

23. Hettinger J, Richards DM, Hansson J, Barra MM, Joschko AC, Krijgsveld J, Feuerer M. Origin of monocytes and macrophages in a committee progenitor. Nat Immunol. 14(2013): 821-830.

24. Murray PJ, Wynn TA. Protective and pathogenic functions of macrophage subsets. Nat Rev Immunol. 11 (2011): 723-737

25. Wheeler AP, Ridley AJ. Why three Rho proteins? RhoA, RhoB, RhoC, and cell motility. Exp Cell Res 301 (2004):43-49.

26. Noguchi T, Koizumi M, Hayashi S. Mitochondria-driven cell elongation mechanism for competing sperms. Fly (Austin). 6(2012):113-6. doi: 10.4161/fly.19862. Epub 2012 Apr 1.

27. Pagliuso A, Cossart P, Stavru. The ever-growing complexity of the mitochondrial fission machinery. Cell Mol Life Sci. 2017 Aug 5. doi: 10.1007/s00018-017-2603-0. [Epub ahead of print]

28. Suen DF, Norris KL, Youle RJ. Mitochondrial dynamics and apoptosis. Genes Dev. 22(2008):1577-1590.

29. Rafelski SM. Mitochondrial network morphology: building an integrative, geometrical view. BMC Biology 11(2013):71-78

30. Hoitzing H, Johnston IG, Jones NS. What is the function of mitochondrial networks? A theoretical assessment of hypotheses and proposal for future research. Bioessays. 37(2015):687-700

31. Friedman JR, Nunnari J. Mitochondrial form and function. Nature. 505(2014):335-343.

32. Vernay A, Marchetti A, Sabra A, Jauslin TN, Rosselin M, Scherer PE, Demaurex N, Orci L, Cosson P. MitoNEET-dependent formation of intermitochondrial junctions. Proc Natl Acad Sci U S A. 114(2017):8277-8282.

33. Chen, H., Detmer, S.A., Ewald, A.J., Griffin, E.E., Fraser, S.E., Chan, D.C. Mitofusins Mfn1 and Mfn2 coordinately regulate mitochondrial fusion and are essential for embryonic development. J. Cell Biol. 160 (2003): 189–200.

Figure legends

Fig.1. The effect of antimycin A and oligomycin A on the morphology of M0 macrophages

Macrophages were immunostained with COX4 antibody and FITC (green)-conjugated secondary antibody to visualize the mitochondria and counterstained with rhodamine-phalloidin (red) to visualize actin and with DAPI (blue) to visualize nuclei. (A, B) Untreated M0 macrophages are elongated with interconnected mitochondria distributed around the nucleus and in the tail. (C, D) M0 macrophages treated with combination of antimycin A and oligomycin A show dramatic shortening and clearly separated, “granular” mitochondria. (E) Graph shows statistically significant difference between the average length of the untreated and treated M0 macrophages. We measured the lengths of several tens of macrophages from independent experiments and averaged the macrophage length. We used T test calculated by Graph pad prism 5 and Excel.Panel A and C are merged images of actin and mitochondrial staining. Panel B and D are merged imaged images of mitochondrial staining and DAPI staining. Bar is equal to 10 μm.

Fig. 2. The effect of antimycin A and oligomycin A on the morphology of M1 macrophages and mitochondrial network

Macrophages were immunostained with COX4 antibody and FITC (green)-conjugated secondary antibody to visualize the mitochondria and counterstained with rhodamine-phalloidin (red) to visualize actin and with DAPI (blue) to visualize the nuclei. (A, C) Untreated M1 macrophages are roundish with a clearly visible network of interconnected mitochondria distributed around the nucleus and in the cell body. (B, D) M1 macrophages treated with a combination of antimycin A and oligomycin A remain roundish but lose their mitochondrial network, and clearly separated “granular” mitochondria are visible. (E) Graph shows that there is no statistically significant difference between the average length of the untreated and treated M1 macrophages. We measured the lengths of several tens of macrophages from independent experiments and averaged the macrophage length. We used T test calculated by Graph pad prism 5 and

Excel.Panel A and B are merged images of mitochondrial and DAPI staining. Panel C and D are merged images of actin and mitochondrial staining. Bar is equal to 10 μm.

Fig. 3. The effect of antimycin A and oligomycin A on the morphology of M2 macrophages

Macrophages were immunostained with COX4 antibody and FITC (green)-conjugated secondary antibody to visualize the mitochondria and counterstained with rhodamine-phalloidin (red) to visualize actin and with DAPI (blue) to visualize the nuclei. (A, B) Untreated M2 macrophages are highly elongated, with a network of interconnected mitochondria distributed around the nucleus and in the tail. (C, D) M2 macrophages treated with combination of Antimycin A and Oligomycin A show dramatic shortening and clearly separated mitochondria. (E) Graph shows statistically significant difference between the average length of the untreated and treated M2 macrophages. We measured the lengths of several tens of macrophages from independent experiments and averaged the macrophage length We used T test calculated by Graph pad prism 5 and Excel. Panel A and C are merged images of actin and mitochondrial staining. Panel B and D are merged images of mitochondrial staining and DAPI staining. Bar is equal to 10 μm.

Fig.4. The effect of antimycin A and oligomycin A on the morphology of RhoA-deleted M0, M1 and M2 macrophages

RhoA-deleted macrophages were immunostained with COX4 antibody and FITC (green)-conjugated secondary antibody to visualize the mitochondria and with DAPI (blue) to visualize nuclei. (A) RhoA-deleted untreated M0 and M2 (B) macrophages are extremely elongated (hummingbird phenotype) with interconnected mitochondria distributed around the nucleus and in the tail. (A1) RhoA-deleted M0 and M2 (B1) macrophages treated with a combination of antimycin A and oligomycin A show dramatic shortening and clearly separated mitochondria. (C) Untreated RhoA-deleted M1 macrophages are roundish/mulipolar with interconnected mitochondria distributed throughout the cytoplasm. (C1) RhoA-deleted M1 macrophages treated with a combination of antimycin A and oligomycin A remain roundish and have clearly separated mitochondria. All panels are merged images of mitochondrial and DAPI staining. Bar is equal to 50 μm.

Fig.5. Western blot analysis of the effect of antimycin A and oligomycin A on the expression of macrophage molecular markers. (A) An example of Western blots from a single experiment. The expression of the M1 marker iNos increases and the expression of M2 marker Arg-1 decreases in macrophages treated with antimycin A in conjunction with oligomycin A. Con- control untreated macrophages, Inh- macrophages treated with inhibitors. Actin was used as a loading control. (B and C) Graphs show the relative expression of iNos and Arg-1 (as compared to actin expression) in the control and inhibitor treated macrophages from 3 independent experiments. P values < 0.05 are statistically significant. We used T test calculated by Graph pad prism 5 and Excel.

Fig.6 The effect of antimycin A and oligomycin A on the ATP, ADP and filamentous (F) and globular (G) actin levels.

Graphs show the average ATP (A) and ADP (B) levels and the ATP/ADP ratio (C) in untreated and inhibitor-treated macrophages calculated from 4 independent experiments. P values < 0.05 are statistically significant. (A). The untreated and treated M2 macrophages have the highest level and the M1 have the lowest level of ATP. The ATP level increases in all macrophage subtypes after treatment with inhibitors. (B) The ADP level in untreated and treated macrophages. The untreated M2 macrophages have the highest level and the M1 have the lowest level of ADP. Inhibitor treatment decreases the level of ADP in all macrophages. (C) The ATP/ADP ratio, which is nearly identical in all subtypes of untreated macrophages, increases after inhibitor treatment. The largest increase occurs in M0 and M2 macrophages and the smallest increase is in M1 macrophages. D) The Western blot of F and G actin in control and inhibitor treated macrophages shows decrease of filamentous- and increase of globular-actin upon inhibitor treatment. E) Graph representation of F and G actin level from three independent blots. The difference between G and F actin is statistically significant at P= 0.0316. We used T test calculated by Graph pad prism 5 and Excel.

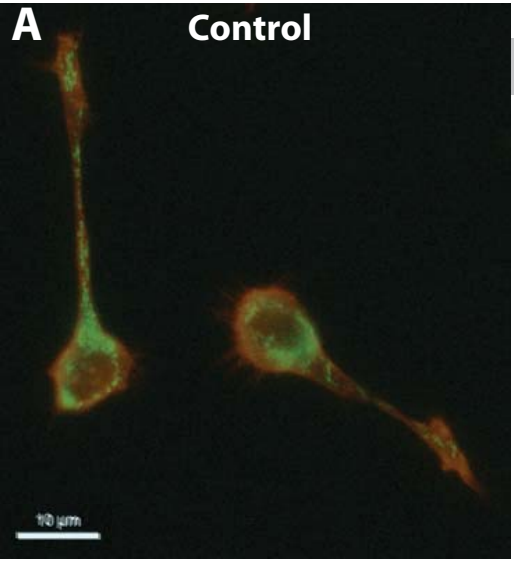
A
Control
10 µm

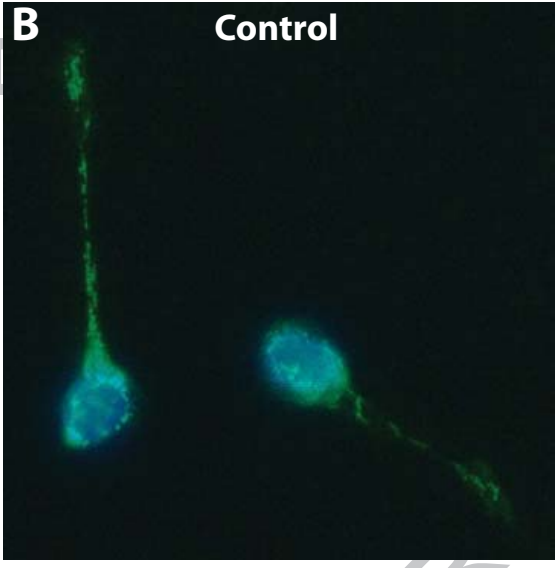
B
Control

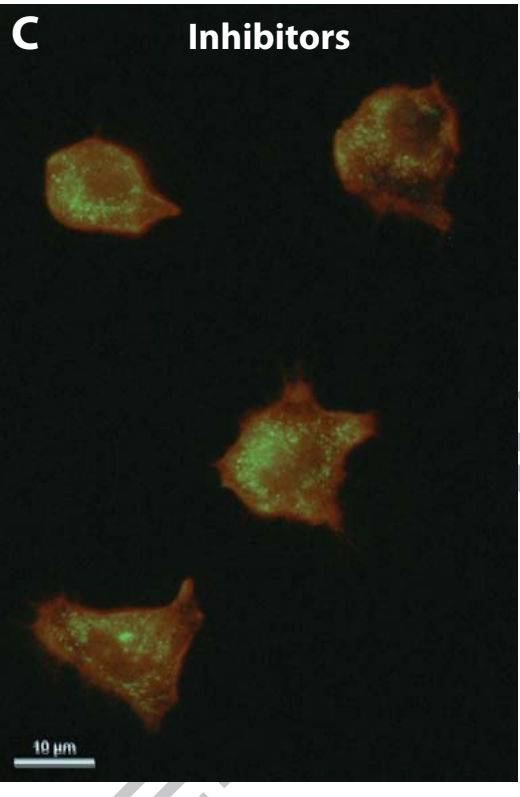
C
Inhibitors
10 µm

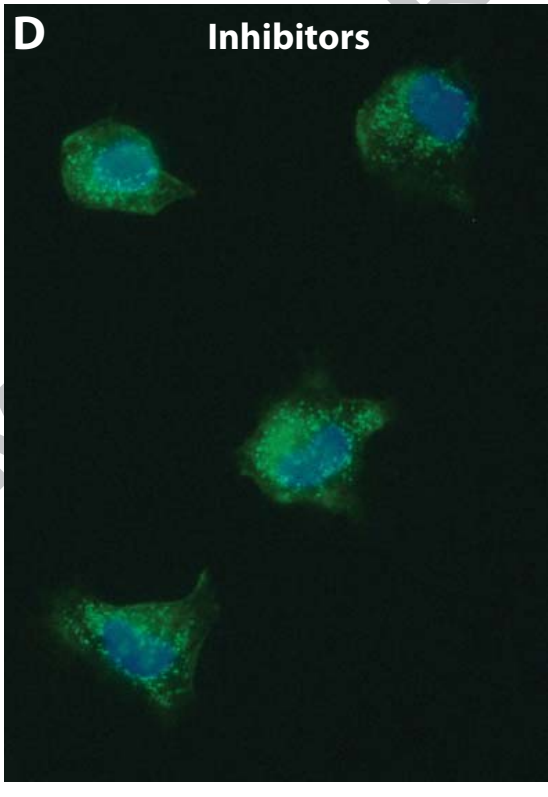
D
Inhibitors

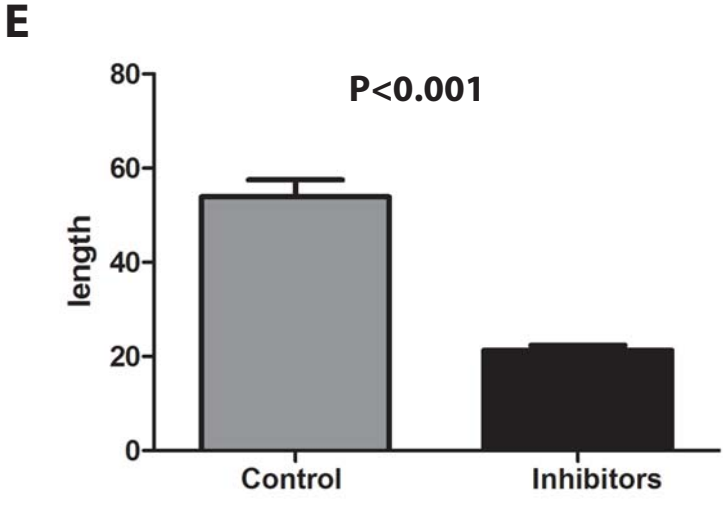
E
P<0.001
80
60
40
20
0
length
Control
Inhibitors

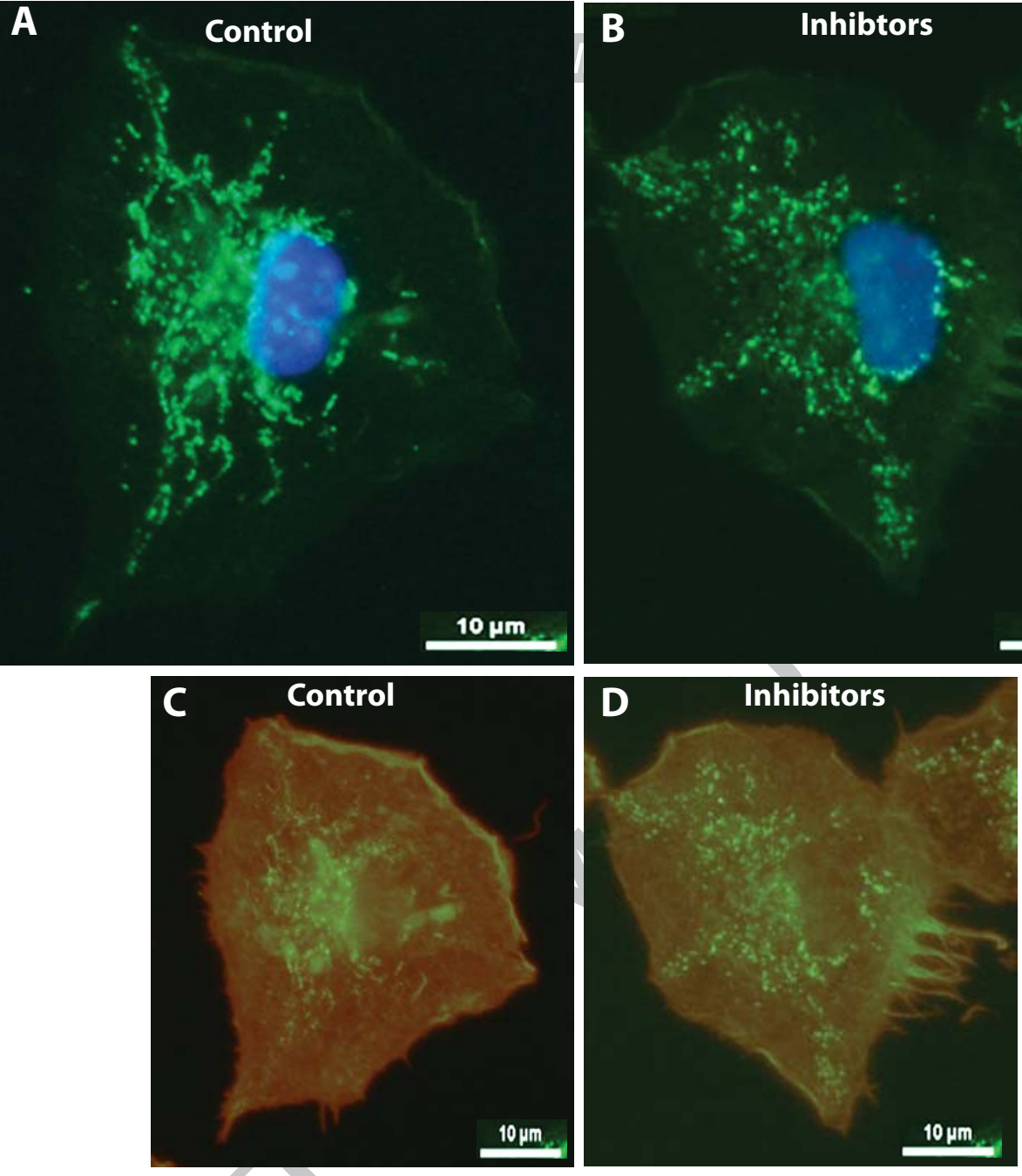
A
Control
10 µm
B
Inhibtors
10 µm

C
Control
10 µm
D
Inhibitors
10 µm

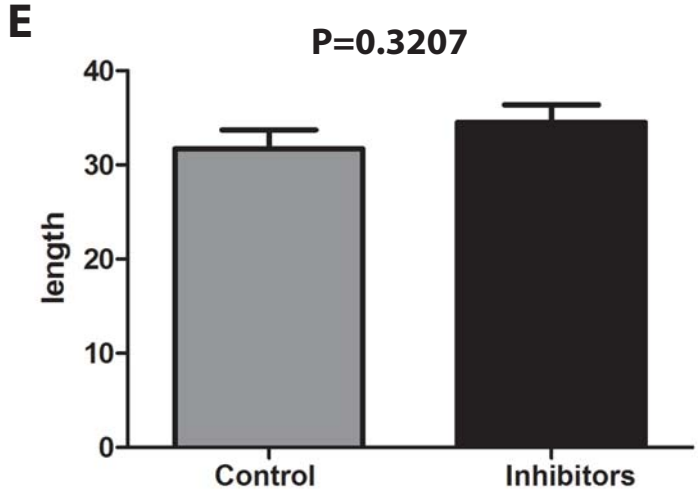
E
P=0.3207
40
30
20
10
0
length
Control
Inhibitors

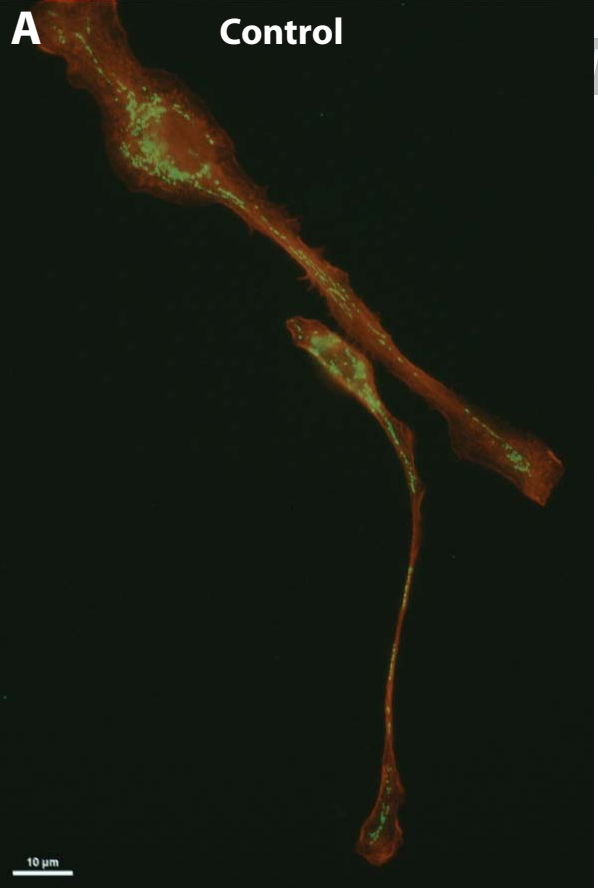
A
Control
10 µm

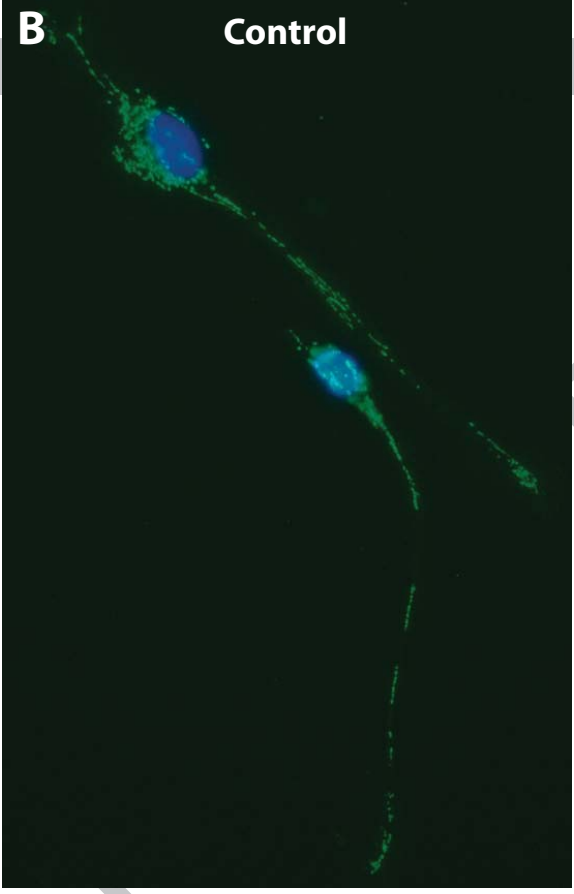
B
Control

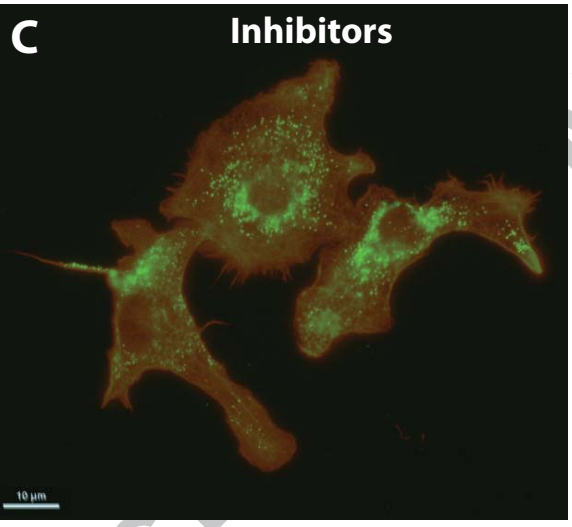
C
Inhibitors
10 µm

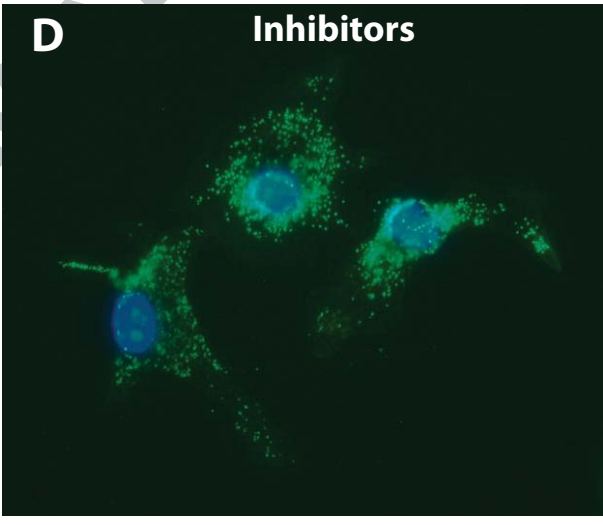
D
Inhibitors


E
P=0.0007
150
100
50
0
length
Control
Inhibitors

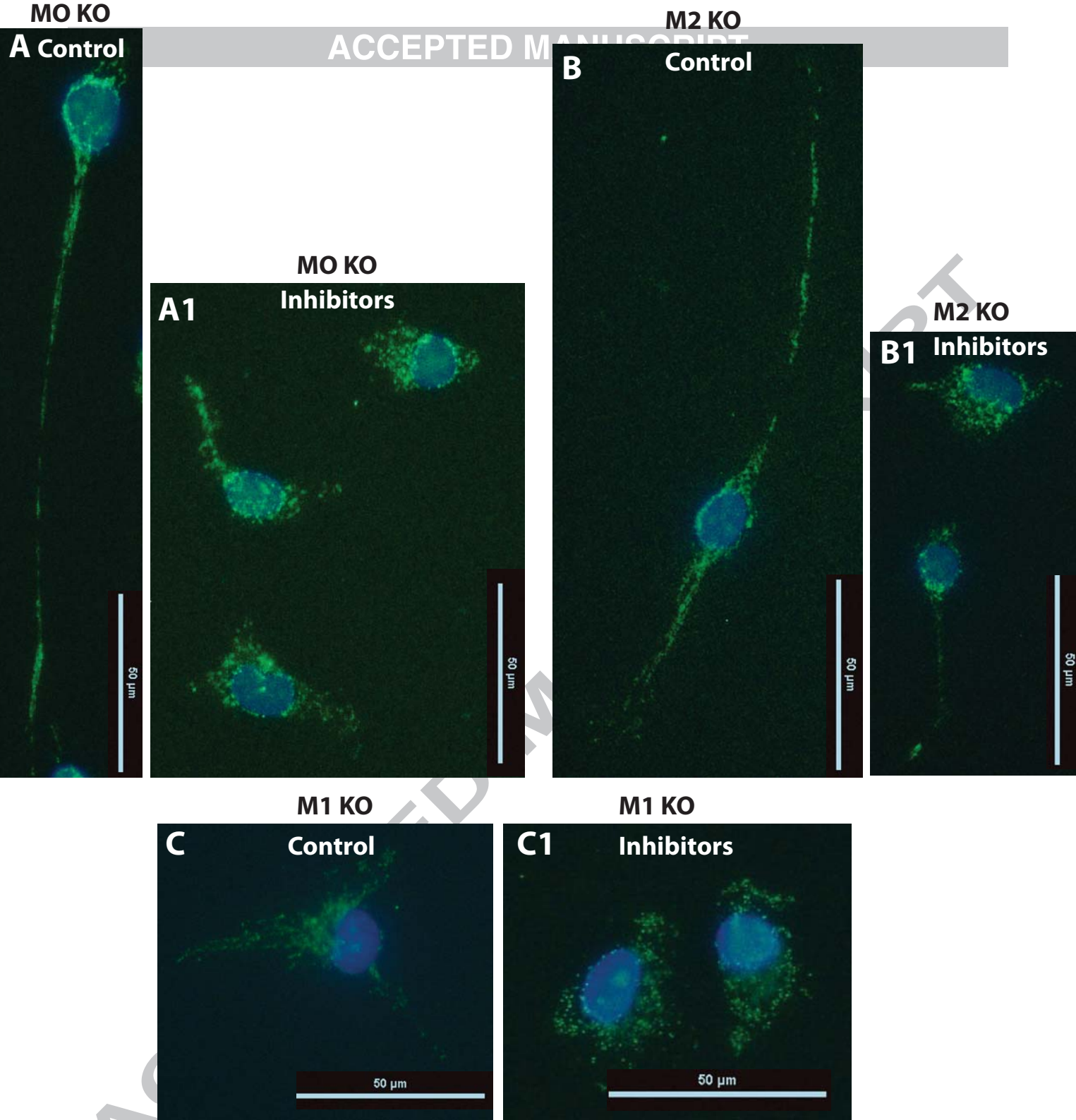

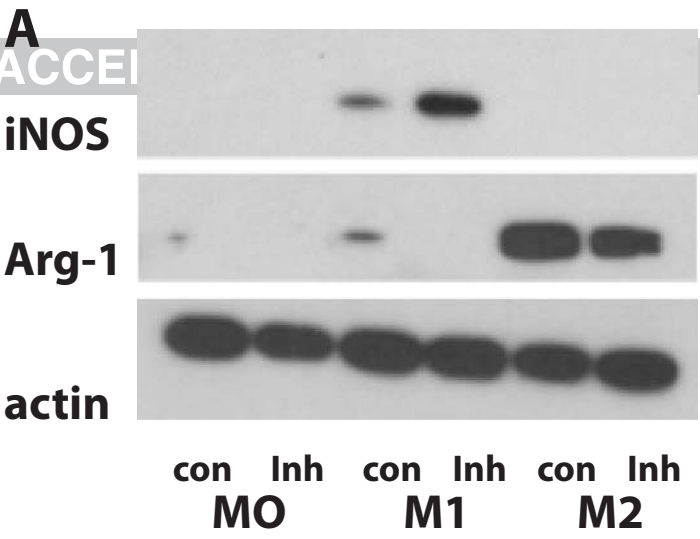

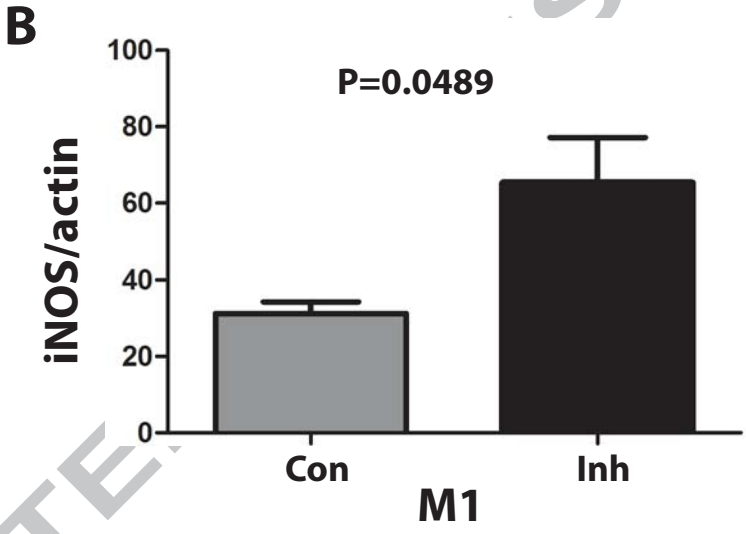

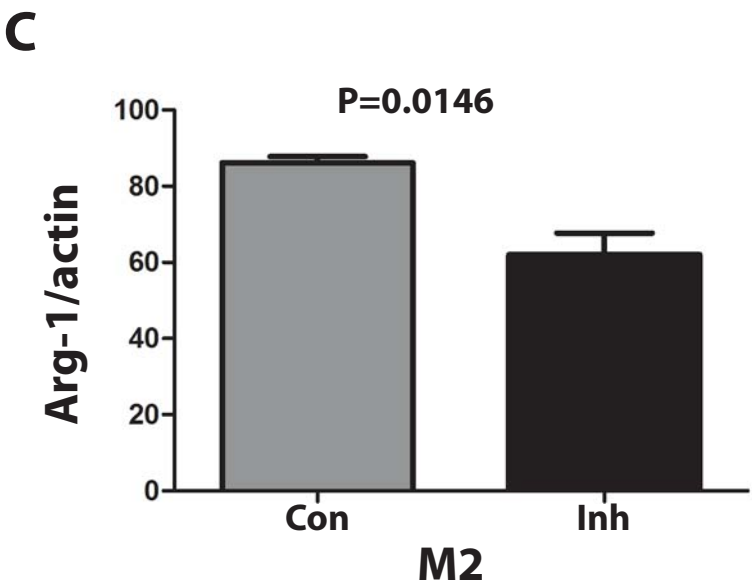

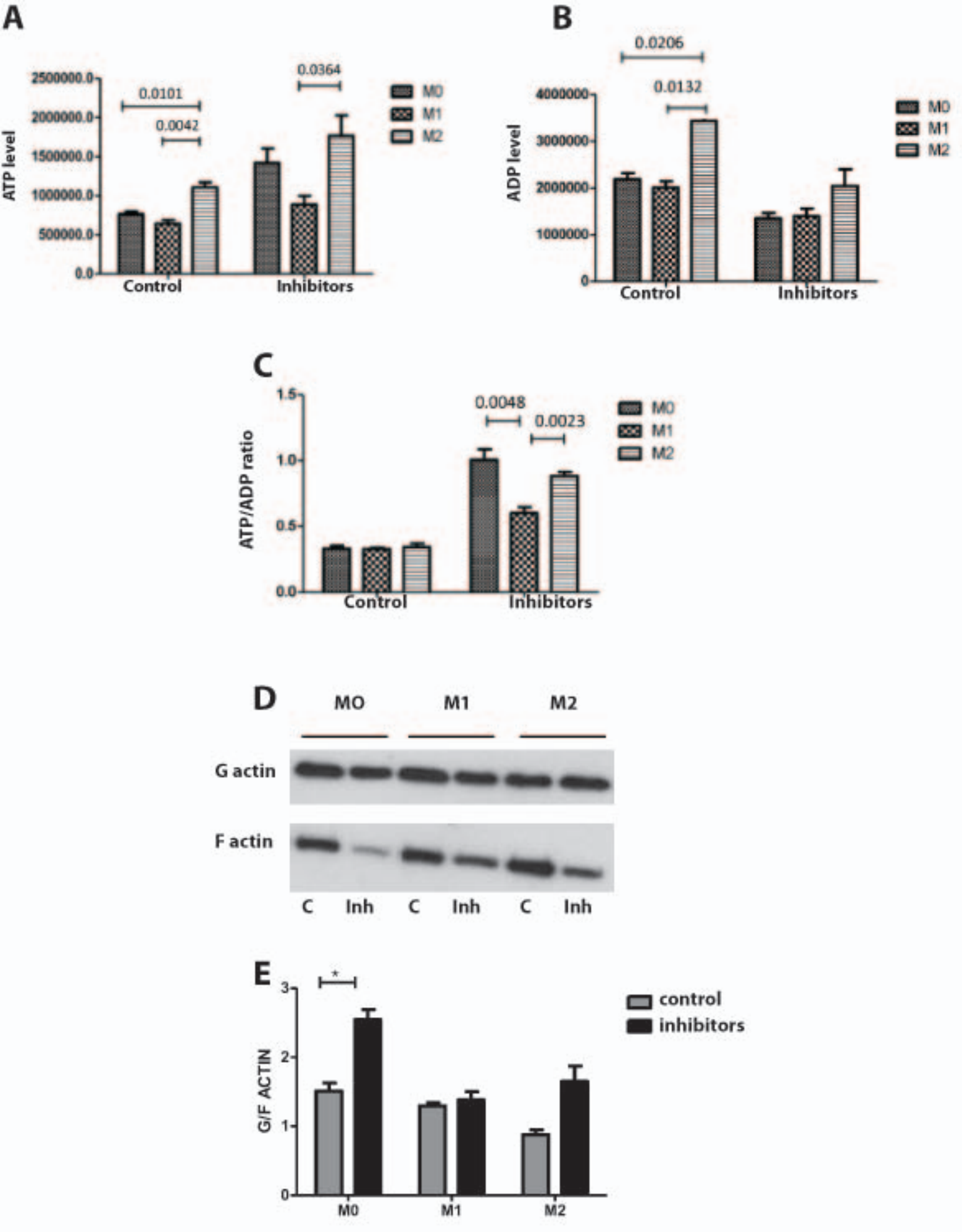
A
ATP level
2500000.0
2000000.0
1500000.0
1000000.0
500000.0
0.0
0.0101
0.0042
0.0364
M0
M1
M2
Control
Inhibitors
B
ADP level
4000000
3000000
2000000
1000000
0
0.0206
0.0132
M0
M1
M2
Control
Inhibitors
C
ATP/ADP ratio
1.5
1.0
0.5
0.0
0.0048
0.0023
M0
M1
M2
Control
Inhibitors
D
MO
M1
M2
G actin
F actin
C
Inh
C
Inh
C
Inh
E
G/F ACTIN
3
2
1
0
*
control
inhibitors
M0
M1
M2

* MO, M1 and M2 macrophage subtypes have different morphologies/shapes and functions.

* We studied the effect of the oxidative phosphorylation inhibitors, antimycin A and oligomycin A, at a suboptimal dose, which depolarizes mitochondria but does not eliminate mitochondrial functions, on the mitochondria/energy production and phenotype of wild-type and RhoA-deleted MO, M1 and M2 peritoneal mouse macrophages.

* Inhibitor treatment resulted in approximately 60% increase in ATP level and ATP/ADP ratio in MO and M2 macrophages, and these changes correlated with a drastic shortening/tail retraction of MO and M2 macrophages, and decreased expression of Arg-1 in M2 macrophages.

* The treatment of M1 macrophages caused only a 30% increase in the ATP level and ATP/ADP ratio, and while it did not affect the shape of M1 macrophages, it increased the production of iNos.

* The maintenance of macrophage phenotypes depends on mitochondrial function and ATP/ADP homeostasis.